Primary and secondary organic aerosols in 2016 summer of Beijing

Rongzhi Tang[1], Zepeng Wu[1], Xiao Li[1], Yujue Wang[1], Dongjie Shang[1], Yao Xiao[1], Mengren Li[1], Limin Zeng[1], Zhijun Wu[1], Mattias Hallquist[2], Min Hu[1], Song Guo[1,*]

[1]*State Key Joint Laboratory of Environmental Simulation and Pollution Control, College of Environmental Sciences and Engineering, Peking University, Beijing, 100871, PR China*

[2] *Atmospheric Science, Department of Chemistry and Molecular Biology, University of Gothenburg, Sweden*

[*] Correspondence to: Song Guo, songguo@pku.edu.cn

Abstract

To improve the air quality, Beijing government has employed several air pollution control measures since 2008 Olympics. In order to investigate the organic aerosol sources after the implementation of these measures, ambient fine particulate matters were collected at a regional site Changping (CP) and an urban site Peking University Atmosphere Environment MonitoRing Station (PKUERS) during the "Photochemical Smog in China" field Campaign in summer of 2016. A chemical mass balance (CMB) modeling and the tracer yield method were used to apportion the primary and secondary organic sources. Our results showed that the particle concentration decreased significantly during the last a few years. The apportioned primary and secondary sources explained 62.8 ± 18.3% and 80.9 ± 27.2% of the measured OC at CP and PKUERS, respectively. Vehicular emissions served as the dominant sources. Except gasoline engine emission, the contributions of all the other primary sources decreased. Besides, the anthropogenic SOC, i.e. toluene SOC, also decreased, implying that deducting primary emission can reduce anthropogenic SOA. Different from the SOA from other regions in the world, where biogenic SOA was dominant, anthropogenic SOA was the major contributor to SOA, implying that deducting anthropogenic VOCs emissions is an efficient way to reduce SOA in Beijing. Back trajectory cluster analysis results showed that high mass concentrations of OC were observed when the air mass was from south. However, the contributions of different primary organic sources were similar, suggesting the regional particle pollution. The ozone concentration and temperature correlated well with the SOA concentration. Different correlations between day and night samples suggested the different SOA formation pathways. Significant enhancement of SOA with increasing particle water content and acidity were observed in our study, suggesting the aqueous phase acid-catalyzed reactions may be the important SOA formation mechanism in summer of Beijing.

1. Introduction

Beijing is the capital and a major metropolis of China. With the rapid economic growth and urbanization, Beijing is experiencing serious air pollution problems, and became one of the hotspots of $PM_{2.5}$ (particular matters with size smaller than 2.5μm) pollution in the world (Guo et al., 2014a; Xiang et al., 2017; Tian et al., 2016). Due to the frequent haze events in Beijing, Beijing government has taken a series of control measures in recent years, especially after 2008 Olympics, which may greatly influence the primary and secondary particle sources. Therefore, elucidating the current contributions of primary particle sources as well as secondary particle sources is of vital importance. It is also important to compare with the previous results to evaluate the effectiveness of the control measures and shed light on the influence of the primary source emission control on the secondary aerosol formation.

Several studies regarding to the source apportionment of fine particles in Beijing have been conducted using multifarious methods during the last few years (Yu et al., 2013; Gao et al., 2014; Zheng et al., 2016b; Tan et al., 2014; Wang et al., 2009; Guo et al., 2013). Receptor model is a commonly used method to apportion the particle sources (Zhang et al., 2017; Zhou et al., 2017; Zhang et al., 2013; Song et al., 2006; Zheng et al., 2005). Elemental tracers were previously used to apportion particulate matter sources (Yu et al., 2013; Gao et al., 2014; Zheng et al., 2016b). However, elemental tracer-based method was unable to distinguish sources that mostly emit organic compounds instead of specific elements such as diesel/gasoline engines. Among all the apportionment methods, chemical mass balance (CMB) model was one of the most commonly used methods to apportion the primary organic sources of fine particulate matter (Zhang et al., 2017; Hu et al., 2015; Schauer et al., 1996). Organic tracers have been successfully used in several studies which aimed to quantify the main sources of Beijing (Liu et al., 2016; Guo et al., 2013; Wang et al., 2009). Wang et al. assessed the source contributions of carbonaceous aerosol during 2005 to 2007 (Wang et al., 2009).

Guo et al. (Guo et al., 2013) and Liu et al. (Liu et al., 2016) apportioned the organic aerosol sources using CMB model in summer of 2008 and a severe haze event in winter of 2013. Both studies found that vehicle emission and coal combustion were the dominant primary sources of fine organic particles. Tracer-yield method has been considered as a useful tool to semi-quantify SOA derived from specific VOCs precursors (Guo et al., 2012; Zhu et al., 2017; Zhu et al., 2016; Tao et al., 2017; Hu et al., 2008). However, only a few studies have estimated secondary organic aerosol in Beijing. Yang et al. (Yang et al., 2016) estimated the biogenic SOC to OC during CAREBEIJING-2007 field campaign, and found that the biogenic SOC accounted for 3.1% of the measured OC. Guo et al. (Guo et al., 2012) illustrated the SOA contributions in 2008, and found that secondary organic carbon could contribute a great portion (32.5 ± 15.9%) to measured organic carbon at the urban site. Ding et al. (Ding et al., 2014) used the tracer-yield method to investigate the SOA loading on a national scale and found that SOA, especially anthropogenic SOA played great role in major city clusters of China.

In this study, we quantified 144 kinds of particulate organic species, including primary and secondary organic tracers, at a regional site and an urban site of Beijing. A CMB modeling and the tracer yield method were used to apportion the primary and secondary sources of the organic aerosols in the 2016 summer of Beijing. The results were compared with the previous studies to evaluate the effectiveness of control measures on primary as well as secondary organic aerosols. Moreover, source apportionment results from different air mass origins according to the back trajectory clustering analysis were shown to investigate the influences of air mass from different directions on the fine organic particle sources. Influencing factors of SOA formation, i.e. temperature, oxidant concentration, aerosol water content, as well as particle acidity were also discussed in this study to improve our understanding of SOA formation under polluted environment.

2. Experimental

2.1 Sampling and Chemical Analysis

The measurements were conducted simultaneously at an urban site Peking University Atmosphere Environment MonitoRing Station (PKUERS, 39°59′21″ N, 116°18′25″ E) and a regional site Changping (CP, 40°8′24″N, 116°6′36″ E) 40km north of PKUERS site during "Photochemical Smog in China" campaign, from May 16th to June 5th, 2016 (see Fig. S1) (Hallquist et al., 2016). The PKUERS site is set on the roof at an academic building on the campus of Peking University in the northwest of Beijing. CP site is located on the fourth floor of a building on the Peking University Changping campus of Changping.

Four-channel samplers (TH-16A, Tianhong, China) consisting of three quartz filter channel and one Teflon filter channel, were employed to collect 12-h aerosol samples at PKUERS and CP, respectively. The sampling flow rate was 16.7 L min^{-1}. Teflon filters were weighed by a microbalance (Toledo AX105DR, USA) after a 24 h balance in an environmental controlled room (temperature 20 ± 1°C, relative humidity 40 ± 3%) for gravimetric analysis. Teflon-based samples were extracted by deionized water to measure water-soluble inorganic compounds (WSICs), namely Na^+, NH_4^+, K^+, Mg^{2+}, Ca^{2+}, NO_3^-, SO_4^{2-} and Cl^- by DIONEX ICS-2500 and ICS-2000 ion-chromatograph. One punch (1.45 cm^2) of quartz-based sample was then cut off to analyze the EC and OC via thermal-optical method using Sunset Laboratory-based instrument (NIOSH protocol, TOT). The other two quartz filters were then extracted and analyzed for chemical composition and particulate organic matters. Some daytime and nighttime samples were combined to ensure the detection of most organic compounds. To better understand the chemical speciation, daytime samples were separated from nighttime samples.

Authentic standards were used to identify and quantify the organic compounds. The analytical methods used in this study referred to the previous work (Song et al., 2014).

Briefly, the samples were first spiked with a mixture of internal standard, including ketopinic acid (KPA), 20 kinds of deuterated compounds, and one carbon isotope ^{13}C-substituted compound. The quartz filters were then ultrasonically extracted with methanol: dichloromethane (v:v=1:3) solvent in water bath (temperature < 30 °C) for 3 times. Each time was 20 min. The extracts were filtered, and then concentrated using a rotary vacuum evaporator. An ultra-pure nitrogen flow was used to further concentrate the extracts into 0.5-1 ml. Each extracted solution was divided into two portions, one of which added BSTFA (BSTFA/TMCS = 99:1, Supelco) to convert polar organic compounds into trimethylsilanized derivatives. Afterwards, the derivatized and the untreated samples were analyzed by an Agilent 6890 GC-MS System (MSD GC-5973N) equipped with an Agilent DB-5MS GC column (30 m × 0.25 mm × 0.5 μm).

2.2 Source Apportionment

A chemical mass balance modelling developed by the U.S. Environmental Protection Agency (EPA CMB version 8.2) was applied to determine the apportion of the primary contribution of OC (Schauer et al., 1996). This receptor model solved a set of linear equations using ambient concentrations and chemical source profiles. CMB approach depends strongly on the representativeness of the source profile. In this study, five primary source profiles including vegetative detritus (Rogge et al., 1993), coal combustion (Zheng et al., 2005), gasoline engines (Lough et al., 2007), diesel engines (Lough et al., 2007) as well as biomass burning (Sheesley et al., 2007) were input into the model. Fitting species including EC，n-alkanes, levoglucosan, 17β(H)-21α(H)-norhopane, 17α(H)-21β(H)-hopane, benzo(b)fluoranthene, benzo(k)fluoranthene, benzo(e)pyrene, benzo(ghi)perylene, indeno(1,2,3-cd)pyrene. The criteria for acceptable fitting results included the square regression coefficient of the regression equation $R^2 > 0.85$ as well as the sum of square residual Chi-square value $\chi^2 < 4$.

The tracer yield method was used to estimate the contributions of biogenic and anthropogenic secondary organic aerosols using fixed tracers to SOC ratio (f_{SOC}) based

on laboratory experiments, which was 0.155 ± 0.039 for isoprene, 0.231 ± 0.111 for α-pinene, 0.0230 ± 0.0046 for β-caryophyllene and 0.0079 ± 0.0026 for toluene (Kleindienst et al., 2007). The mass fraction depends on the degree of oxidation. Besides, the uncertainty also depends on the selection of molecular tracers and the simplified procedures by using single-valued mass fractions (Yttri et al., 2011; El Haddad et al., 2011; Song et al., 2014; Guo et al., 2014b; Guo et al., 2014c). Previous studies showed that SOA estimated by the tracer-yield method and POA apportioned by CMB model could fully account for the OA in atmospheric atmosphere (Lewandowski et al., 2008; Kleindienst et al., 2010). Besides, researchers found that the total estimated SOC derived from tracer-yield method was in accordance with the that stemmed from EC-tracer method during summer (Ding et al., 2012; Kleindienst et al., 2010; Turpin and Huntzicker, 1995). Comparable results were also found between tracer-yield method and positive matric factorization model (Hu et al., 2010; Zhang et al., 2009). All these results firmly demonstrated that the tracer-yield method is a valuable and convincing method to estimate the SOA contributions (Ding et al., 2014).

Estimations based on boundary values were generally acknowledged to have the largest source of uncertainties in the models, so those results could be used to determine the possible limit of the estimations. Also, Kleindienst et al. carried out a boundary analysis using the data from North California to measure the range of estimated SOA contributions. Results revealed that the possible contributions of isoprene, α-pinene, β-caryophyllene and toluene were within the scope of 70-130%, 50-220%, 70-120% and 60-160%, respectively. The above results were supposed to be in the acceptable range for PM2.5 source apportionment. Besides, the standard deviations of the tracer-to-SOC ratios were suitable as a source profile uncertainty (Kleindienst et al., 2007). Despite the uncertainties above, tracer-yield represented a unique approach to estimate the SOA contributions using individual hydrocarbon precursors up to now.

3. Gaseous pollutants and particle chemical composition

3.1 Gaseous pollutants and meteorological conditions of the observation period

Mixing ratios of gaseous pollutants and meteorological conditions during the observation period were shown in Fig. S2 and Table S1. Compared with the results in summer of 2010 (Zheng et al., 2016a), the gaseous mixing ratios SO_2 and CO were lower than before owing to the desulfurization efforts made by the government. Higher concentrations of NO and NO_2 were caused by the increasing number of vehicles. The increment of ozone indicated the importance of secondary pollution. Clearly, ozone concentration at CP was higher than that of PKUERS while other pollutants were lower.

During the campaign, the average wind speed was low, showing average values of 2.3 ± 1.4 m/s and 2.4 ± 1.5 m/s at CP and PKUERS, respectively. The diurnal variations of wind directions and speeds are exhibited in Fig. S2. The prevailing wind was from south, with higher wind speed during the daytime.

To explore the influence of the air masses from different directions on fine particle loading and sources, back trajectory analysis was performed using National Oceanic and Atmospheric Administration (NOAA) Hybrid Single Particle Lagrangian Integrated Trajectory (HYSPLIT) model. We calculated 36 h air mass back trajectories arriving at two sampling site during the observation period using the HYSPIT-4 model with a 1°×1° latitude-longitude grid and the final meteorological database. The model was run with the starting time of 0:00, 4:00, 8:00, 12:00, 16:00, and 20:00 UTC). The arrival level was set at 200 m above ground level. The method used in trajectory clustering was based on GIS-based software TrajStat (http://www.meteothinker.com/TrajStatProduct.aspx). 36-h back trajectories staring at 200 m above ground level in CP and PKUERS were calculated every 4 hours during the entire campaign and then clustered according to their similarity in spatial distribution using the HYSPLIT4 software. Three-cluster solution was adopted as shown in Fig. S3. The three clusters were defined as Far North West (Cluster 1, Far

NW), Near West North (Cluster2, Near WN), and South (Cluster 3). South cluster was found to be the most frequent one, accounting for 52% at CP and 64% at PKUERS. Clusters Far NW and Near NW accounted for 17% and 31%, 17% and 19% at CP and PKUERS, respectively.

3.2 Overview of $PM_{2.5}$ chemical composition

In this study, daily $PM_{2.5}$ concentrations fluctuated dramatically from 6.7 μg m^{-3} to 80.3 μg m^{-3} at CP, and from 9.6 to 82.5 μg m^{-3} at PKUERS, respectively. A paired t-test was used to compare the mass concentrations at two sites. The results indicate that the mass concentrations showed statistically non-significant difference, suggesting the regional particle pollution in Beijing. $PM_{2.5}$ mass concentrations during the summer of 2008 to 2016 in Beijing are summarized in Table 1. Guo et al. (Guo et al., 2013) reported the average $PM_{2.5}$ concentrations during the summers of 2000 to 2008, which showed distinct decreasing tendency during 2000-2006 and then slightly increased in 2007 due to unfavorable meteorological conditions. To better understand the variation tendency of the $PM_{2.5}$ in the summer of Beijing, we compared the fine particle matter data since 2008. Compared with 2008, the $PM_{2.5}$ concentrations decreased from 92.3 ± 44.7 μg m^{-3} to 88.2 μg m^{-3} in 2009 and 62.7 μg m^{-3} in 2010. The mass concentration continued falling to 45.5 μg m^{-3} in 2016. This decreasing is attributed to the drastic emission control measures implemented by the Beijing government since 2012. In spite of the prominent decrease of the $PM_{2.5}$ mass concentrations, the aerosol loading in Beijing was still much higher than that in developed countries (Tai et al., 2010; Barmpadimos et al., 2012; Park and Cho, 2011).

Fig. S4 showed the chemical composition of $PM_{2.5}$. In general, organic particulate matters (OM, OC*1.6) and sulfate were the two dominant components, accounting for more than 50% of the $PM_{2.5}$ mass concentration during the field campaign. The average concentration of total WSICs for CP was 17.4 ± 11.5 μg m^{-3}, higher than that of PKUERS (12.2 ± 8.5μg m^{-3}). Among the WSICs, secondary inorganic ions (sulfate,

nitrate, and ammonium) were the most abundant compounds, indicating secondary particles played great roles in the summer of Beijing. The higher sulfate proportion could be explained by the increased photochemical conversion of sulfur dioxide to sulfate aerosol (Xiang et al., 2017). Relevant data of main WSICs (sulfate, nitrate and ammonia) during 2008 to 2016 were also included in table 1 to better elucidate the drastic decrease of fine particulate matter in recent years. Results showed that the daily average concentration of WSICs decreased from 2008 to 2016, with sulfate decreased from 35.6 μg/m^3 to 4.7 μg/m^3, nitrate decreased from 7.9 μg/m^3 to 2.4 μg/m^3, ammonia decreased from 15.2 μg/m^3 to 3.5 μg/m^3. The significant decrease of WSICs confirmed the effectiveness of the control measures taken by the government.

Carbonaceous aerosols, i.e. organic carbon (OC) and elemental carbon (EC) were also great contributors to $PM_{2.5}$ concentrations. Higher proportion of OC and EC at PKUERS demonstrated severe carbonaceous pollution in urban Beijing, which might have close correlation with the higher traffic flow, coal/wood combustion by residents and industrial emissions (Wang et al., 2006; Dan et al., 2004; Cao et al., 2004). Comparison of the OC, EC concentrations from 2008 to 2016 were also listed in Table 1. Unlike $PM_{2.5}$, OC concentration at PKUERS showed a higher OC concentration (11.0 ± 3.7 μg m^{-3}) compared with that in 2008 (9.2 ± 3.3μg m^{-3}), suggesting organic aerosol pollution becomes more and more important. EC concentration decreased dramatically to 0.7 ± 0.5 μg m^{-3} at CP and 1.8 ± 1.0 μg m^{-3} at PKUERS, which showed the lowest value since 2000. This could be attributed to the implementation of air pollution prevention and control action plan enacted by the state council since 2013. Therefore, we could draw a conclusion that the drastic decrease of fine particulate matter in Beijing was mainly due to the well-controlled EC and WSICs, with negligible contribution of OC.

To evaluate the influences of the air masses from different directions on the $PM_{2.5}$ loadings during the campaign, three categories were divided according to the back trajectory clustering analysis (See Fig. S5). In general, cluster south represented the

most polluted air mass origin followed by clusters Near WN and Far NW, which was in accordance with previous studies demonstrating severe aerosol pollution in southerly air flow in summer of Beijing (Huang et al., 2010; Sun et al., 2010).

3.3 Concentration of particulate organic species from different air mass origins

The organic species (except secondary organic tracers) were divided into 12 categories. Their concentrations in different directions according to the back trajectory clustering were shown in Fig. S6. Detailed information for each class at the two sites could be found in the supplementary material (Fig. S7). Cluster south showed higher particulate organic matter concentration, followed by cluster near WN and far NW, indicating more severe aerosol pollution from the south. Our result consists with the previous studies that more pollution emissions are from the south area of Beijing than those from the north (Wu et al., 2011; Zhang et al., 2009).

For all the species, the histogram showed the daily average concentrations with error bars representing one standard deviation. Dicarboxylic acid was the most abundant species among all the components, demonstrating the great contribution of the secondary formation to the organic aerosols in the summer of Beijing (Guo et al., 2010). A series of n-alkanes ranging from C12 to C36 were analyzed. Their distribution during the observation period was shown in Fig. S7 (a). The maximum-alkane concentration species (C_{max}) were C27 and C29. The odd carbon preference was an indicative of biogenic sources (vegetative matters and biomass burning) (Huang et al., 2006; Rogge et al., 1993). In this study, total PAHs were much lower than previous studies in summer of Beijing, suggesting the effectiveness of the control strategies since 2013 (Wang et al., 2009). According to Fig. S7 (c), five ring PAHs were dominant species among all the species, followed by four-ring and six-ring PAHs. In total, four to six ring PAHs had higher abundancy, accounting for more than 60% of the total PAHs. The result was much similar with previous studies that the distribution of PAHs was impacted by the volatility of PAHs and the temperature (Wang et al., 2009; Guo et al., 2013). Saccharide

was considered to originate from biomass burning (Simoneit et al., 1999). In this study, we quantified three sugar compounds including levoglucosan, manosan and galactosan, in which levoglucosan was considered as a good tracer for biomass burning. The average daily mass concentration of levoglucosan at CP and PKUERS were 53.03 ± 39.26 ng m^{-3} and 59.87 ± 38.93 ng m^{-3}, respectively. It's worth mentioning that the levoglucosan concentration was the lowest in recent years (Cheng et al., 2013; Guo et al., 2013). Hopanes have been considered as markers for oil combustion (Lambe et al., 2009), vehicles (i.e. gasoline-powered and diesel-powered engine) (Cass, 1998; Lough et al., 2007) and coal combustion (Oros and Simoneit, 2000). Nevertheless, contributions of coal combustion to hopanes were much less than that of vehicle exhaustion. Concentrations of quantified hopanes including 17α(H)-22,29,30-trishopane, 17β(H)-21α(H)-norhopane, and 17α(H)-21β(H)-hopane of CP and PKUERS are shown in Fig. S7(d). The total average concentrations of hopanes were 3.05 ± 1.53 ng m^{-3} for CP and 3.90 ± 2.06 ng m^{-3} for PKUERS. The daily averaged hopanes concentrations at urban site PKUERS were much higher than that of CP, which could probably explained by the heavier vehicle emissions in the urban area. The concentrations of primary organic tracers used in CMB model were listed in Table S2.

3.4 Biogenic and anthropogenic SOA tracers

Table S3 compared the SOA tracers measured in this work with those in other regions in the world as well as that observed in Beijing 2008. The sites for comparison include an urban background site at Indian Institute of Technology Bombay, Mumbai, India (IITB) (Fu et al., 2016), an outflow region of Asian aerosols and precursors Cape Hedo, Okinawa, Japan (CH) (Zhu et al., 2016), a residential site at Yuen Long, Hong Kong (YL) (Hu et al., 2008), three industrial sites at Cleveland Ohio (CL, data was averaged among the three sites), a suburban site in the Research Triangle Park North California (RTP). The detailed information about these sites were summarized in the supplementary material.

Three isoprene-SOA tracers i.e. two 2-methyltetrols (2-methyltheitol and 2-methylerythritol) and 2-methylglyceric acid were detected. The summed concentration of the isoprene-SOA tracers ranged from 3.7 to 62.3 ng m^{-3} at CP and 8.6 to 46.5 ng m^{-3} at PKUERS. The concentration was higher than that of IITB and CH. Compared with the isoprene-SOA tracers in 2008, the concentrations in 2016 were lower.

Nine α-pinene tracers were identified. The sum of the tracers ranged from 20.9 to 282.3 ng m^{-3} at CP and 50.0 to 161.4 ng m^{-3} at PKUERS, which had similar distribution pattern with that measured in 2008 Beijing and YL. The total α-pinene tracer concentrations were lower than those in 2008, while still much higher than the concentrations in other regions of the world.

β-caryophyllinic acid is one of the oxidation products of β-caryophyllene which is considered as a tracer for β-caryophyllene SOA. In this study, β-caryophyllinic acid concentrations ranged from 1.4 to 16.7 ng m^{-3} at CP, and 0.9 to 12.0 ng m^{-3} at PKUERS, with average daily average concentrations of 6.1 ± 3.5 ng m^{-3} and 6.0 ± 2.8 ng m^{-3} for CP and PKUERS, respectively. The values were lower than those at YL and RPT, higher than that measured at Yufa and PKUERS in 2008.

2,3-Dihydroxy-4-oxopentanoic acid is deemed as a tracer for toluene SOA. Our results showed that the 2,3-Dihydroxy-4-oxopentanoic acid concentration was 9.7 ± 7.3 ng m^{-3} at CP and 11.0 ± 3.7 ng m^{-3} at PKUERS. Compared with other regions of the world, the concentrations of 2,3-Dihydroxy-4-oxopentanoic acid was much higher, implying higher contributions of anthropogenic sources at Beijing. However, the 2,3-dihydroxy-4-oxopentanoic acid concentrations in CP were lower than that of PKUERS.

4. Primary sources and secondary formation of organic aerosols

4.1 Contributions of primary and secondary organic aerosols

A CMB model and the tracer-yield method were used to quantify the contributions of primary and secondary sources to the ambient organic carbon (See Fig. 1). On average,

the primary sources accounted for 42.6 ± 15.4% and 50.4 ± 19.1% of the measured OC at CP and PKUERS, respectively. The vehicle emissions were the dominant primary sources, with the contributions of 28.8 ± 14.8% and 37.6 ± 19.3% at PKUERS and CP, respectively, implying the urgency to control vehicular exhaustion in urban areas. Despite of the lower contribution of the gasoline exhaust at PKUERS, the mass concentration of the gasoline exhaust was higher compared with that of CP given the higher OC loading at PKUERS. The contributions of biomass burning were 3.9 ± 2.6% and 5.0 ± 2.2% at CP and PKUERS, respectively, showing the higher concentrations at night. The drastic change of the biomass burning contribution in CP at night was due to occasional burning activities at night. Coal combustion contributed 5.8 ± 5.5% and 4.6 ± 2.6% of the measured OC at CP and PKUERS. The higher contribution at CP was due to more burning activities in the suburban areas.

The secondary organic sources accounted for 20.2 ± 6.7% of the organic carbon at CP, with 1.6 ± 0.4% from isoprene, 4.4 ± 1.5% from α-pinene, 2.7 ± 1.0% from β-caryophyllene and 12.5 ± 3.4% from toluene. As for PKUERS, the secondary organic sources took up 30.5 ± 12.0% of the measured OC, in which isoprene was responsible for 2.3 ± 0.9%, α-pinene for 5.6 ± 1.9%, β-caryophyllene for 3.6 ± 2.6% and toluene for 19.0 ± 8.2%. Haque et al. (Haque et al., 2016) used tracer-based method to apportion the organic carbon and results showed that the biogenic SOC was responsible for 21.3% of the total OC with isoprene SOC contributing 17.4%, α/β-pinene SOC contributing 2.5% and β-caryophyllene SOC contributing 1.4% in the summer of Alaska, implying the significant contributions of the biogenic SOA to the loading of the organic aerosol. Our results exhibited that the biogenic SOA concentration was comparable or even high than that at some forest sites in other places of the world (Miyazaki et al., 2012; Stone et al., 2012; Claeys et al., 2004; Kourtchev et al., 2008). The SOA formation mechanism is complicated. A possible reason is the high oxidation capacity in China. Higher oxidation capacity in China may fasten the chemical lifetime of reactive gases and accelerate the aerosol aging process which leads to an increase in biogenic SOA

(Ghirardo et al., 2016). Another possible reason derived from the complicated emissions of anthropogenic VOCs which can lead to an enhancement of secondary organic aerosol formation from biogenic precursors (Hoyle et al., 2011). We also compare the isoprene concentration with the forest site according to some literatures. Wang et al. (Wang et al., 2010) discovered that the mean isoprene concentration was 0.24 ppbv at PKUERS in June 2008. Lappalainen et al. (Lappalainen et al., 2009) measured the isoprene concentration of the boreal forest in Hyytiala and found that the mean concentration of isoprene was 0.15 ppbv. This comparable, or even higher concentration of isoprene may be due to different sources of biogenic VOCs. More work is still needed to investigate the SOA formation mechanism under Air Pollution Complex in China.

Stone et al. (Stone et al., 2009) discovered that primary and secondary sources accounted for 83 ± 8% of the measured organic carbon, with primary sources accounted for 37 ± 2% and SOC contributed for 46 ± 6% with 16 ± 2% from biogenic gas-phase precursors and 30 ± 4% from toluene using CMB model and tracer-based method at Cleveland with heavy industries, implying that anthropogenic sources played great roles in the formation of SOA. Our results showed a similar with the results published by Stone et al., where anthropogenic sources i.e. toluene derived SOC dominated the apportioned SOC. Our research revealed an important point that controlling SOA seems feasible in the developing countries like China. It is difficult to control SOA in developed countries, since biogenic SOA are dominant. However, deducting anthropogenic precursors may be an efficient way to reduce the SOA pollution where anthropogenic SOA is dominant. On average, 62.8 ± 18.3% and 80.9 ± 27.2% of the measured OC were apportioned at CP and PKUERS, respectively. About 36.3 ± 18.1% and 29.3 ± 15.6% of the OC sources remained unknown, which were probably composed of uncharacterized primary or secondary sources. Further research is needed to explain the unapportioned sources of OC.

Due to the drastic emission control measures taken by the Beijing government, the primary and secondary sources in Beijing may change greatly. Fig. 2 displayed the comparison of the sources between 2008 and 2016 at the same site PKUERS. We compared the average contributions by percentage rather than the mass concentration. In general, primary sources contributed 50.4 ± 19.1% of the measured OC in 2016, closely correlated to the increasing contribution of vehicular emissions. Gasoline engines accounted for 18% of the measured OC, showing an enhancement of 80% with respect to 2008. This might be related to the rising number of the vehicles in Beijing. In comparison, diesel exhaust decreased by 12.5% due to the strict control measures made by the government. A 28.5% and 20% reduction of coal combustion and biomass burning could also be found due to the drastic measures made by the government. Compared with 2008, contributions of secondary organic aerosol decreased by 29.4%, in which biogenic SOC served as the biggest contributor to this decreasing. The formation of biogenic SOA is complicated. Several factors can affect biogenic SOC formation, among which the precursor concentration is one of the crucial factors. Biogenic VOCs, i.e. isoprene, α-pinene etc. are predominantly emitted from plant foliage in a constitutive manner. The emission rate of biogenic VOCs depends on various factors, e.g. radiation, temperature, humidity, meteorological conditions and seasonality (Ghirardo et al., 2016). Two or more of them will act synergistically to have an effect on the concentration of isoprene SOC. Besides, the changes of the vegetation in certain area may also play a part in the change of the SOC concentration. Considering its comprehensive synergistic effect, it's difficult to determine the main reason responsible for the isoprene SOC decrease.

However, the contribution of toluene SOC was the highest among the apportioned SOC, which was different from the results of the most developed countries in the world. Compared with previous studies, except β-caryophyllene SOC, vegetative detritus and gasoline exhausts, the contributions of all other sources decreased, e.g. isoprene SOC, α-pinene SOC, toluene SOC, biomass burning, diesel exhaust, and coal combustion.

However, the increases in β-caryophellene SOC, vegetative detritus and gasoline exhausts could not compensate for the decreases of other sources. This can be attributed to the larger portion of uncharacterized sources compared with 2008. The uncharacterized sources may mainly contain cooking emissions, mineral and road dust, industrial pollution as well as other uncharacterized secondary sources (Tian et al., 2016; Liu et al., 2016). In summary, the contributions of most POA decreased in recent years, except for gasoline exhaust, indicating more efforts should be made to control the gasoline emission. The apportioned SOC was also decreased with toluene SOC served as the dominant source. Our results revealed that deducting anthropogenic precursors may be an efficient way to control SOA pollution in China.

4.2 Organic aerosol sources from different air mass origins

The regional sources and transport of air pollutants exert profound impacts on air quality of Beijing. To better understand the regional impacts on the primary and secondary aerosol sources of Beijing, source apportionment results when air mass from different origins were shown in Fig. 3. Vehicular emissions i.e. gasoline and diesel exhaust showed identical contributions from different air mass origins (31.0% from south vs 31.3% from Near WN vs 31.7% from Far NW) at PKUERS, demonstrating the vehicular pollution could mostly be attributed to the vehicular emission at the local site. However, the contribution of vehicular emission at CP showed significant difference from different air mass origins, with lowest contribution when air mass was from far northwest. This might be explained by regional transport from different directions. Comparable contributions of coal combustion and biomass burning were found at CP and PKUERS from different air mass origins, implying the regional pollution in Beijing. Similarly, biogenic SOC showed similar contributions from different air mass origins both at the regional site and the urban site. From all the directions, the toluene SOC (anthropogenic source) was the largest contributor to apportioned SOC, with higher concentrations at the urban site PKUERS. On the whole,

most of the sources showed comparable contribution from different air mass origins, implying the pollution in Beijing was regional.

4.3 Influencing factors for secondary organic aerosol formation in the summer of Beijing

Laboratory experiments have revealed that several factors can influence the SOA formation, e.g. oxidants (OH radical, ozone etc.), temperature, humidity, particle water content and acidity. We found that the correlations between SOC and ozone/temperature are different for daytime and nighttime samples. However, it's not significant for water content and hydrogen ions concentration. Therefore, we separate the data between day and night between SOC and ozone/temperature, and use entire data for the analysis of particle water and acidity. In this work, the relationships between estimated SOA and these factors were investigated to better understand the SOA formation in Beijing.

SOA formation from ozonolysis

Ozone is considered as an important oxidant for SOA formation. Fig. 4 (a)(b) showed the correlation with ozone mixing ratio and SOC. It is clear that SOC increased significantly with the increasing of ozone mixing ratio, which is consistent with previous studies in Beijing (Guo et al. 2012). Different correlations were found between day and night samples, with better correlation for the daytime samples at both sites, implying SOA may have other formation mechanism at night other than ozonolysis. At CP, the growth rate of SOC with O_3 was similar for day and night samples, which was 0.02 μg m^{-3} per ppbv ozone. For PKUERS, the increment rate of the SOC towards ozone was 0.04 μg $m^{-3}$and 0.02 μg m^{-3} per ppbv ozone at day and night, respectively.

Influence of temperature and relative humidity on SOA formation

Temperature was considered as a great influencing factor on SOA formation. On the one hand, higher temperature promoted the evaporation of the semi volatile SOA. On the other hand, high-temperature conditions would favor the oxidation, which would

accelerate the SOA formation (Saathoff et al., 2009). Fig. 4 (c) (d) showed the variation of SOC concentrations with the temperature. In this study, SOC concentration showed positive correlation with temperature at CP and PKUERS, demonstrating that temperature favors the SOA formation in the summer of Beijing. Moreover, different correlation of the day and the night samples imply the different pathways of SOA formation. However, poor relations could be found between SOC and RH.

Effects of aqueous-phase acid catalyzed reactions on SOA formation

Aerosol water and acidity have been considered to have great impact on the aqueous-phase SOA formation (Cheng et al., 2016). To figure out the influences of water content and aerosol acidity on the aqueous-phase reactions, ISORROPIA-II thermodynamic equilibrium model was used (Surratt et al., 2007). The model was set at forward mode, based on the concentrations of particle phase Na^+, NH_4^+, K^+, Mg^{2+}, Ca^{2+}, NO_3^-, SO_4^{2-}, Cl^- and gaseous NH_3 as well as ambient temperature and RH.

Results showed that the average aerosol water content at CP was 3.87 ± 3.73 μg m^{-3}, higher than that at PKUERS (1.83 ± 1.81 μg m^{-3}). The water content was lower in 2016 than that in 2008. The estimated SOC concentration showed good correlations with water content at both sites. Compared with CP, the correlation factor in PKUERS was better, implying that aqueous phase reaction may be more important in the urban area. Different correlation could be found at different liquid water contents, especially for CP, where liquid water contented spanned a wide range, implying that different mechanisms may exist at different liquid water content.

In this study, modeled H^+ concentration and SOC showed significant correlation ($p<0.05$) at the two places, which indicated that acid-catalyzed reaction might provide a crucial pathway for the SOA formation in the summer of Beijing. Laboratory studies showed that acid-catalyzed reactive uptake might play great role in the enhancement of SOA (Zhang et al., 2014; Surratt et al., 2010; Jang et al., 2002). However, contrary conclusions were made by other group, demonstrating the inconsistence of the aerosol

acidity and the SOA formation (Wong et al., 2015; Kristensen et al., 2014). The contradiction might give the facts that the impacts of the acidity on the SOA loading varied from place to place, determined by the specific environmental conditions. Linear regression showed that the enhancement of SOC with modeled H^+ concentration were at a value of 0.02 μg m^{-3} per nmol H^+, which was lower than the previous results (0.046 for PKUERS, and 0.041 for Yufa, 2008). Offenberg et al. (Offenberg et al., 2009) discovered good correlation between SOC and $[H^+]_{air}$, with R^2 value of 0.815. Besides, a one nmol m^{-3} $[H^+]_{air}$ would give rise to 0.015 μg m^{-3} SOC increase from the oxidation of α-pinene in the chamber experiment. We also analyzed the relationship between apportioned SOC and sulfate concentration and found that the apportioned SOC increased with the increase of sulfate concentration. The coefficient R^2 were 0.41 and 0.45 for CP and PKUERS, respectively, indicating that the increase of SOC may be influenced by the sulfate aerosol. As such, the increase in SOC is likely arise from the acid-catalyzed reactions with the participation of sulfate aerosols. In the present work, different correlations could be found at different modeled H^+ concentrations where apportioned SOC increased significantly as the H^+ concentration increased and then increased slowly at a certain level, showing gradient growth at different hydrogen-ion concentrations. Therefore, aqueous phase acid-catalyzed reactions may influence the SOA formation through different mechanisms at varied level of liquid water concentration and aerosol acidity.

5. Conclusion

High concentrations of fine particles were observed during the "Campaign on Photochemical Smog in China", with the average mass concentrations of 45.48 ± 19.78 μg m^{-3} and 42.99 ± 17.50 μg m^{-3}, at CP site and PKUERS site, respectively. Compared with previous studies, the concentrations of $PM_{2.5}$, EC and estimated SOC decreased significantly, due to the drastic measures implemented by the government in the recent years. However, OC showed a higher concentration, suggesting particulate organic matters become more and more important in Beijing. CMB modeling and tracer-yield

514 method were used to apportion the primary and secondary organic aerosol sources. The
515 apportioned primary and secondary OC accounted for 62.8 ± 18.3% and 80.9 ± 27.2%
516 of the measured OC at CP and PKUERS, respectively. Vehicle emissions i.e. diesel and
517 gasoline engine emissions were the major primary organic aerosol sources, which
518 contributed to 28.8 ± 14.8% and 37.6 ± 19.3% of the OC at CP and PKUERS,
519 respectively. Compared with the results of the previous work, the gasoline engine
520 emission contributed almost twice of that in 2008 (18.0% vs 10.0%), while the
521 contribution of diesel engine emission decreased by 12.5% compared with the result in
522 2008. Besides, the contributions of biomass burning and coal combustion both
523 decreased. The apportioned biogenic and anthropogenic SOC can explain 20.2 ± 6.7%
524 and 30.5 ± 12.0% of the measured OC at CP and PKUERS, respectively. The
525 contribution of toluene SOC is the highest among the apportioned SOC, which is
526 different from the results of the most developed countries in the world. Our results
527 revealed an important point, which is that controlling SOA seems feasible in the
528 developing countries like China. It is difficult to control SOA in developed countries,
529 since biogenic SOA are dominant. However, deducting anthropogenic precursors may
530 be an efficient way to reduce the SOA pollution where anthropogenic SOA is dominant.
531 Back trajectory clustering analysis showed that the particle source contributions were
532 similar when air masses were from different directions, suggesting the regional organic
533 particle pollution in Beijing. However, the higher organic particle loading from south
534 cluster indicates that there were more emissions from southern region of Beijing. The
535 present work also implied that the aqueous phase acid-catalyzed reactions may be an
536 important SOA formation mechanism in summer of Beijing.

Acknowledgement

This research is supported by the National Key R&D Program of China (2016YFC0202000, Task 3), the National Natural Science Foundation of China (21677002), framework research program on 'Photochemical smog in China' financed by Swedish Research Council (639-2013-6917).

References

Barmpadimos, I., Keller, J., Oderbolz, D., Hueglin, C., and Prévôt, A.: One decade of parallel fine ($PM_{2.5}$) and coarse (PM_{10}–$PM_{2.5}$) particulate matter measurements in Europe: trends and variability, Atmos Chem Phys, 12, 3189-3203, 2012.

Cao, J. J., Lee, S. C., Ho, K. F., Zou, S. C., Fung, K., Li, Y., Watson, J. G., and Chow, J. C.: Spatial and seasonal variations of atmospheric organic carbon and elemental carbon in Pearl River Delta Region, China, Atmospheric Environment, 38, 444t-4456, http://doi.org/10.1016/j.atmosenv.2004.05.016, 2004.

Cass, G. R.: Organic molecular tracers for particulate air pollution sources, Trac-Trends in Analytical Chemistry, 17, 356-366, 10.1016/s0165-9936(98)00040-5, 1998.

Cheng, Y., Engling, G., He, K. B., and Duan, F. K.: Biomass burning contribution to Beijing aerosol, Atmospheric Chemistry & Physics, 13, 7765-7781, 2013.

Cheng, Y., Zheng, G., Wei, C., Mu, Q., Zheng, B., Wang, Z., Gao, M., Zhang, Q., He, K., and Carmichael, G.: Reactive nitrogen chemistry in aerosol water as a source of sulfate during haze events in China, Science Advances, 2, e1601530, 2016.

Claeys, M., Graham, B., Vas, G., Wang, W., Vermeylen, R., Pashynska, V., Cafmeyer, J., Guyon, P., Andreae, M. O., and Artaxo, P.: Formation of Secondary Organic Aerosols Through Photooxidation of Isoprene, Science, 303, 1173, 2004.

Dan, M., Zhuang, G., Li, X., Tao, H., and Zhuang, Y.: The characteristics of carbonaceous species and their sources in PM2.5 in Beijing, Atmospheric Environment, 38, 3443-3452, http://doi.org/10.1016/j.atmosenv.2004.02.052, 2004.

Ding, X., Wang, X. M., Gao, B., Fu, X. X., He, Q. F., Zhao, X. Y., Yu, J. Z., and Zheng, M.: Tracer‐based estimation of secondary organic carbon in the Pearl River Delta, south China, Journal of Geophysical Research Atmospheres, 117, 2012.

Ding, X., He, Q. F., Shen, R. Q., Yu, Q. Q., and Wang, X. M.: Spatial distributions of secondary organic aerosols from isoprene, monoterpenes, beta-caryophyllene, and

aromatics over China during summer, Journal of Geophysical Research-Atmospheres, 119, 11877-11891, 10.1002/2014jd021748, 2014.

El Haddad, I., Marchand, N., Temime-Roussel, B., Wortham, H., Piot, C., Besombes, J. L., Baduel, C., Voisin, D., Armengaud, A., and Jaffrezo, J. L.: Insights into the secondary fraction of the organic aerosol in a Mediterranean urban area: Marseille, Atmos Chem Phys, 11, 2059-2079, 2011.

Fu, P., Aggarwal, S. G., Chen, J., Li, J., Sun, Y., Wang, Z., Chen, H., Liao, H., Ding, A., Umarji, G. S., Patil, R. S., Chen, Q., and Kawamura, K.: Molecular Markers of Secondary Organic Aerosol in Mumbai, India, Environ. Sci. Technol., 50, 4659-4667, 10.1021/acs.est.6b00372, 2016.

Gao, J. J., Tian, H. Z., Cheng, K., Lu, L., Wang, Y. X., Wu, Y., Zhu, C. Y., Liu, K. Y., Zhou, J. R., Liu, X. G., Chen, J., and Hao, J. M.: Seasonal and spatial variation of trace elements in multi-size airborne particulate matters of Beijing, China: Mass concentration, enrichment characteristics, source apportionment, chemical speciation and bioavailability, Atmospheric Environment, 99, 257-265, 10.1016/j.atmosenv.2014.08.081, 2014.

Ghirardo, A., J. Xie, X. Zheng, Y. Wang, R. Grote, K. Block, J. Wildt, T. Mentel, A. Kiendler-Scharr, and M. Hallquist (2016), Urban stress-induced biogenic VOC emissions and SOA-forming potentials in Beijing, Atmospheric chemistry and physics, 16(5), 2901-2920.

Guo, S., Hu, M., Wang, Z. B., Slanina, J., and Zhao, Y. L.: Size-resolved aerosol water-soluble ionic compositions in the summer of Beijing: implication of regional secondary formation, Atmos Chem Phys, 10, 947-959, 2010.

Guo, S., Hu, M., Guo, Q., Zhang, X., Zheng, M., Zheng, J., Chang, C. C., Schauer, J. J., and Zhang, R.: Primary Sources and Secondary Formation of Organic Aerosols in Beijing, China, Environmental Science & Technology, 46, 9846-9853, 10.1021/es20425641, 2012.

596 Guo, S., Hu, M., Guo, Q., Zhang, X., Schauer, J., and Zhang, R.: Quantitative evaluation
597 of emission controls on primary and secondary organic aerosol sources during
598 Beijing 2008 Olympics, Atmos Chem Phys, 13, 8303-8314, 2013.
599 Guo, S., Hu, M., Zamora, M. L., Peng, J., Shang, D., Zheng, J., Du, Z., Wu, Z., Shao,
600 M., and Zeng, L.: Elucidating severe urban haze formation in China, Proceedings
601 of the National Academy of Sciences, 111, 17373-17378, 2014a.
602 Guo, S., Hu, M., Guo, Q. F., and Shang, D. J.: Comparison of Secondary Organic
603 Aerosol Estimation Methods, Acta Chim Sinica, 72, 658-666,
604 10.6023/A14040254, 2014b.
605 Guo, S., Hu, M., Shang, D., Guo, Q., and Hu, W.: Research on Secondary Organic
606 Aerosols Basing on Field Measurement, Acta Chim. Sinica, 72, 145-157, DOI:
607 10.6023/A13111169, 2014c.
608 Haque, M. M., Kawamura, K., and Kim, Y.: Seasonal variations of biogenic secondary
609 organic aerosol tracers in ambient aerosols from Alaska, Atmospheric
610 Environment, 130, 95-104, 10.1016/j.atmosenv.2015.09.075, 2016.
611 Hoyle, C., Boy, M., Donahue, N., Fry, J., Glasius, M., Guenther, A., Hallar, A., Huff
612 Hartz, K., Petters, M., and Petäjä, T.: A review of the anthropogenic influence on
613 biogenic secondary organic aerosol, Atmospheric Chemistry and Physics, 11, 321-
614 343, 2011.
615 Hu, D., Bian, Q., Li, T. W., Lau, A. K., and Yu, J. Z.: Contributions of isoprene,
616 monoterpenes, β-caryophyllene, and toluene to secondary organic aerosols in
617 Hong Kong during the summer of 2006, Journal of Geophysical Research:
618 Atmospheres, 113, 2008.
619 Hu, D., Bian, Q., Lau, A. K. H., and Yu, J. Z.: Source apportioning of primary and
620 secondary organic carbon in summer PM2.5 in Hong Kong using positive matrix
621 factorization of secondary and primary organic tracer data, Journal of Geophysical
622 Research Atmospheres, 115, 2010

623 Hu, M., Guo, S., Peng, J.-f., and Wu, Z.-j.: Insight into characteristics and sources of
624 PM2. 5 in the Beijing–Tianjin–Hebei region, China, National Science Review, 2,
625 257-258, 2015.
626 Huang, X.-F., He, L.-Y., Hu, M., and Zhang, Y.-H.: Annual variation of particulate
627 organic compounds in PM 2.5 in the urban atmosphere of Beijing, Atmospheric
628 Environment, 40, 2449-2458, 2006.
629 Huang, X. F., He, L. Y., Hu, M., Canagaratna, M. R., Sun, Y., Zhang, Q., Zhu, T., Xue,
630 L., Zeng, L. W., and Liu, X. G.: Highly time-resolved chemical characterization
631 of atmospheric submicron particles during 2008 Beijing Olympic Games using an
632 Aerodyne High-Resolution Aerosol Mass Spectrometer, Atmospheric Chemistry
633 & Physics Discussions, 10, 8933-8945, 2010.
634 Jang, M. S., Czoschke, N. M., Lee, S., and Kamens, R. M.: Heterogeneous atmospheric
635 aerosol production by acid-catalyzed particle-phase reactions, Science, 298, 814-
636 817, 10.1126/science.1075798, 2002.
637 Kleindienst, T. E., Jaoui, M., Lewandowski, M., Offenberg, J. H., Lewis, C. W., Bhave,
638 P. V., and Edney, E. O.: Estimates of the contributions of biogenic and
639 anthropogenic hydrocarbons to secondary organic aerosol at a southeastern US
640 location, Atmospheric Environment, 41, 8288-8300, 2007.
641 Kleindienst, T., MichaelLewandowski, Offenberg, J., Edney, E., MohammedJaoui,
642 MeiZheng, XiangDing, and Edgerton, E.: Contribution of Primary and Secondary
643 Sources to Organic Aerosol and PM2.5 at SEARCH Network Sites, Journal of the
644 Air & Waste Management Association, 60, 1388, 2010.
645 Kourtchev, I., Warnke, J., Maenhaut, W., Hoffmann, T., and Claeys, M.: Polar organic
646 marker compounds in PM2.5 aerosol from a mixed forest site in western Germany,
647 Chemosphere, 73, 1308-1314, 2008.
648 Kristensen, K., Cui, T., Zhang, H., Gold, A., Glasius, M., and Surratt, J.: Dimers in α-
649 pinene secondary organic aerosol: effect of hydroxyl radical, ozone, relative
650 humidity and aerosol acidity, Atmos Chem Phys, 14, 4201-4218, 2014.

Lambe, A. T., Miracolo, M. A., Hennigan, C. J., Robinson, A. L., and Donahue, N. M.: Effective Rate Constants and Uptake Coefficients for the Reactions of Organic Molecular Markers (n-Alkanes, Hopanes, and Steranes) in Motor Oil and Diesel Primary Organic Aerosols with Hydroxyl Radicals, Environ. Sci. Technol., 43, 8794-8800, 10.1021/es901745h, 2009.

Lappalainen, H., Sevanto, S., Bäck, J., Ruuskanen, T., Kolari, P., Taipale, R., Rinne, J., Kulmala, M., and Hari, P.: Day-time concentrations of biogenic volatile organic compounds in a boreal forest canopy and their relation to environmental and biological factors, Atmospheric Chemistry and Physics, 9, 5447-5459, 2009.

Lewandowski, M., Jaoui, M., Offenberg, J. H., Kleindienst, T. E., Edney, E. O., Sheesley, R. J., and Schauer, J. J.: Primary and secondary contributions to ambient PM in the midwestern United States, Environmental Science & Technology, 42, 3303-3309, 2008.

Liu, Q. Y., Baumgartner, J., Zhang, Y., and Schauer, J. J.: Source apportionment of Beijing air pollution during a severe winter haze event and associated pro-inflammatory responses in lung epithelial cells, Atmospheric Environment, 126, 28-35, 10.1016/j.atmosenv.2015.11.031, 2016.

Lough, G. C., Christensen, C. G., Schauer, J. J., Tortorelli, J., Mani, E., Lawson, D. R., Clark, N. N., and Gabele, P. A.: Development of molecular marker source profiles for emissions from on-road gasoline and diesel vehicle fleets, J. Air Waste Manage. Assoc., 57, 1190-1199, 10.3155/1047-3289.57.10.1190, 2007.

Hallquist, M., Munthe, J., Hu, M., Wang, T., Chan, C. K., Gao, J., Boman, J., Guo, S., Hallquist, Å. M., and Mellqvist, J.: Photochemical smog in China: scientific challenges and implications for air-quality policies, National Science Review, 3, 401-403, 2016.

Miyazaki, Y., Jung, J., Fu, P., Mizoguchi, Y., Yamanoi, K., and Kawamura, K.: Evidence of formation of submicrometer water-soluble organic aerosols at a deciduous

forest site in northern Japan in summer, Journal of Geophysical Research: Atmospheres, 117, 2012.

Offenberg, J. H., Lewis, C. W., Lewandowski, M., Jaoui, M., Kleindienst, T. E., and Edney, E. O.: Contributions of toluene and alpha-pinene to SOA formed in an irradiated toluene/alpha-pinene/NO(x)/ air mixture: comparison of results using 14C content and SOA organic tracer methods, Environmental Science & Technology, 41, 3972-3976, 2007.

Offenberg, J. H., Lewandowski, M., Edney, E. O., Kleindienst, T. E., and Jaoui, M.: Influence of Aerosol Acidity on the Formation of Secondary Organic Aerosol from Biogenic Precursor Hydrocarbons, Environ. Sci. Technol., 43, 7742-7747, 10.1021/es901538e, 2009.

Oros, D. R., and Simoneit, B. R. T.: Identification and emission rates of molecular tracers in coal smoke particulate matter, Fuel, 79, 515-536, Doi 10.1016/S0016-2361(99)00153-2, 2000.

Park, S. S., and Cho, S. Y.: Tracking sources and behaviors of water-soluble organic carbon in fine particulate matter measured at an urban site in Korea, Atmospheric environment, 45, 60-72, 2011.

Rogge, W. F., Hildemann, L. M., Mazurek, M. A., Cass, G. R., and Simoneit, B. R. T.: Sources of fine organic aerosol. 4. Particulate abrasion products from leaf surfaces of urban plants, Environ. Sci. Technol., 27, 2700-2711, 1993.

Saathoff, H., Naumann, K.-H., Möhler, O., Jonsson, Å. M., Hallquist, M., Kiendler-Scharr, A., Mentel, T. F., Tillmann, R., and Schurath, U.: Temperature dependence of yields of secondary organic aerosols from the ozonolysis of α-pinene and limonene, Atmos Chem Phys, 9, 1551-1577, 2009.

Schauer, J. J., Rogge, W. F., Hildemann, L. M., Mazurek, M. A., Cass, G. R., and Simoneit, B. R. T.: Source apportionment of airborne particulate matter using organic compounds as tracers, Atmospheric Environment, 30, 3837-3855, 10.1016/1352-2310(96)00085-4, 1996.

706 Sheesley, R. J., Schauer, J. J., Zheng, M., and Wang, B.: Sensitivity of molecular
707 marker-based CMB models to biomass burning source profiles, Atmospheric
708 Environment, 41, 9050-9063, 2007.
709 Simoneit, B. R., Schauer, J. J., Nolte, C., Oros, D. R., Elias, V. O., Fraser, M., Rogge,
710 W., and Cass, G. R.: Levoglucosan, a tracer for cellulose in biomass burning and
711 atmospheric particles, Atmospheric Environment, 33, 173-182, 1999.
712 Song, G., Min, H., Qingfeng, G., and Dongjie, S.: Comparison of secondary organic
713 aerosol estimation methods, ACTA CHIMICA SINICA, 72, 658-666, 2014.
714 Song, Y., Zhang, Y., Xie, S., Zeng, L., Zheng, M., Salmon, L. G., Shao, M., and Slanina,
715 S.: Source apportionment of PM2. 5 in Beijing by positive matrix factorization,
716 Atmospheric Environment, 40, 1526-1537, 2006.
717 Stone, E. A., Nguyen, T. T., Pradhan, B. B., and Dangol, P. M.: Assessment of biogenic
718 secondary organic aerosol in the Himalayas, Environmental Chemistry, 9, 263-272,
719 2012.
720 Sun, J., Zhang, Q., Canagaratna, M. R., Zhang, Y., Ng, N. L., Sun, Y., Jayne, J. T., Zhang,
721 X., Zhang, X., and Worsnop, D. R.: Highly time- and size-resolved
722 characterization of submicron aerosol particles in Beijing using an Aerodyne
723 Aerosol Mass Spectrometer, Atmospheric Environment, 44, 131-140, 2010.
724 Surratt, J. D., Kroll, J. H., Kleindienst, T. E., Edney, E. O., Claeys, M., Sorooshian, A.,
725 Ng, N. L., Offenberg, J. H., Lewandowski, M., Jaoui, M., Flagan, R. C., and
726 Seinfeld, J. H.: Evidence for organosulfates in secondary organic aerosol, Environ.
727 Sci. Technol., 41, 517-527, 10.1021/es062081q, 2007.
728 Surratt, J. D., Chan, A. W., Eddingsaas, N. C., Chan, M., Loza, C. L., Kwan, A. J.,
729 Hersey, S. P., Flagan, R. C., Wennberg, P. O., and Seinfeld, J. H.: Reactive
730 intermediates revealed in secondary organic aerosol formation from isoprene,
731 Proceedings of the National Academy of Sciences, 107, 6640-6645, 2010.
732 Tai, A. P., Mickley, L. J., and Jacob, D. J.: Correlations between fine particulate matter
733 (PM 2.5) and meteorological variables in the United States: Implications for the

734 sensitivity of PM 2.5 to climate change, Atmospheric Environment, 44, 3976-3984,
735 2010.
736 Tan, J. H., Duan, J. C., Chai, F. H., He, K. B., and Hao, J. M.: Source apportionment of
737 size segregated fine/ultrafine particle by PMF in Beijing, Atmospheric Research,
738 139, 90-100, 10.1016/j.atmosres.2014.01.007, 2014.
739 Tao, J., Zhang, L., Cao, J., Zhong, L., Chen, D., Yang, Y., Chen, D., Chen, L., Zhang,
740 Z., Wu, Y., Xia, Y., Ye, S., and Zhang, R.: Source apportionment of PM2.5 at urban
741 and suburban areas of the Pearl River Delta region, south China - With emphasis
742 on ship emissions, Science of the Total Environment, 574, 1559-1570,
743 10.1016/j.scitotenv.2016.08.175, 2017.
744 Tian, S. L., Pan, Y. P., and Wang, Y. S.: Size-resolved source apportionment of
745 particulate matter in urban Beijing during haze and non-haze episodes, Atmos
746 Chem Phys, 16, 1-19, 10.5194/acp-16-1-2016, 2016.
747 Turpin, B. J., and Huntzicker, J. J.: Identification of secondary organic aerosol episodes
748 and quantitation of primary and secondary organic aerosol concentrations during
749 SCAQS, Atmospheric Environment, 29, 3527-3544, 1995.
750 Wang, B., Shao, M., Lu, S., Yuan, B., Zhao, Y., Wang, M., Zhang, S., and Wu, D.:
751 Variation of ambient non-methane hydrocarbons in Beijing city in summer 2008,
752 Atmospheric Chemistry and Physics, 10, 5911, 2010.
753 Wang, Q., Shao, M., Zhang, Y., Wei, Y., Hu, M., and Guo, S.: Source apportionment of
754 fine organic aerosols in Beijing, Atmospheric Chemistry and Physics, 9, 8573-
755 8585, 2009.
756 Wang, X., Bi, X., Sheng, G., and Fu, J.: Chemical composition and sources of PM10
757 and PM2. 5 aerosols in Guangzhou, China, Environmental Monitoring and
758 Assessment, 119, 425-439, 2006.
759 Wong, J. P. S., Lee, A. K. Y., and Abbatt, J. P. D.: Impacts of Sulfate Seed Acidity and
760 Water Content on Isoprene Secondary Organic Aerosol Formation, Environ. Sci.
761 Technol., 49, 13215-13221, 10.1021/acs.est.5b02686, 2015.

762 Wu, Y., Guo, J., Zhang, X., and Li, X.: Correlation between PM concentrations and
763 Aerosol Optical Depth in eastern China based on BP neural networks, Geoscience
764 and Remote Sensing Symposium, 2011, 5876-5886.
765 Xiang, P., Zhou, X. M., Duan, J. C., Tan, J. H., He, K. B., Yuan, C., Ma, Y. L., and
766 Zhang, Y. X.: Chemical characteristics of water-soluble organic compounds
767 (WSOC) in PM2.5 in Beijing, China: 2011-2012, Atmos. Res., 183, 104-112,
768 10.1016/j.atmosres.2016.08.020, 2017.
769 Yang, F., Kawamura, K., Chen, J., Ho, K. F., Lee, S. C., Gao, Y., Cui, L., Wang, T. G.,
770 and Fu, P. Q.: Anthropogenic and biogenic organic compounds in summertime fine
771 aerosols (PM2.5) in Beijing, China, Atmospheric Environment, 124, 166-175,
772 10.1016/j.atmosenv.2015.08.095, 2016.
773 Yttri, K. E., Simpson, D., Nojgaard, J. K., Kristensen, K., Genberg, J., Stenstrom, K.,
774 Swietlicki, E., Hillamo, R., Aurela, M., Bauer, H., Offenberg, J. H., Jaoui, M., Dye,
775 C., Eckhardt, S., Burkhart, J. F., Stohl, A., and Glasius, M.: Source apportionment
776 of the summer time carbonaceous aerosol at Nordic rural background sites, Atmos
777 Chem Phys, 11, 13339-13357, 2011.
778 Yu, L. D., Wang, G. F., Zhang, R. J., Zhang, L. M., Song, Y., Wu, B. B., Li, X. F., An,
779 K., and Chu, J. H.: Characterization and Source Apportionment of PM2.5 in an
780 Urban Environment in Beijing, Aerosol Air Qual Res, 13, 574-583,
781 10.4209/aaqr.2012.07.0192, 2013.
782 Zhang, H., Zhang, Z., Cui, T., Lin, Y.-H., Bhathela, N. A., Ortega, J., Worton, D. R.,
783 Goldstein, A. H., Guenther, A., Jimenez, J. L., Gold, A., and Surratt, J. D.:
784 Secondary Organic Aerosol Formation via 2-Methyl-3-buten-2-ol Photooxidation:
785 Evidence of Acid-Catalyzed Reactive Uptake of Epoxides, Environmental Science
786 & Technology Letters, 1, 242-247, 10.1021/ez500055f, 2014.
787 Zhang, Q., Streets, D. G., Carmichael, G. R., He, K. B., Huo, H., Kannari, A., Klimont,
788 Z., Park, I. S., Reddy, S., Fu, J. S., Chen, D., Duan, L., Lei, Y., Wang, L. T., and

Yao, Z. L.: Asian emissions in 2006 for the NASA INTEX-B mission, Atmos Chem Phys, 9, 5131-5153, 2009.

Zhang, R., Jing, J., Tao, J., Hsu, S.-C., Wang, G., Cao, J., Lee, C. S. L., Zhu, L., Chen, Z., and Zhao, Y.: Chemical characterization and source apportionment of PM 2.5 in Beijing: seasonal perspective, Atmos Chem Phys, 13, 7053-7074, 2013.

Zhang, Y. X., Sheesley, R. J., Schauer, J. J., Lewandowski, M., Jaoui, M., Offenberg, J. H., Kleindienst, T. E., and Edney, E. O.: Source apportionment of primary and secondary organic aerosols using positive matrix factorization (PMF) of molecular markers, Atmospheric Environment, 43, 5567-5574, 2009.

Zhang, Y., Cai, J., Wang, S., He, K., and Zheng, M.: Review of receptor-based source apportionment research of fine particulate matter and its challenges in China, The Science of the total environment, 586, 917-929, 10.1016/j.scitotenv.2017.02.071, 2017.

Zheng, J., Hu, M., Peng, J., Wu, Z., Kumar, P., Li, M., Wang, Y., and Guo, S.: Spatial distributions and chemical properties of PM 2.5 based on 21 field campaigns at 17 sites in China, Chemosphere, 159, 480-487, 2016a.

Zheng, M., Salmon, L. G., Schauer, J. J., Zeng, L., Kiang, C., Zhang, Y., and Cass, G. R.: Seasonal trends in PM2. 5 source contributions in Beijing, China, Atmospheric Environment, 39, 3967-3976, 2005.

Zheng, X. X., Guo, X. Y., Zhao, W. J., Shu, T. T., Xin, Y. A., Yan, X., Xiong, Q. L., Chen, F. T., and Lv, M.: Spatial variation and provenance of atmospheric trace elemental deposition in Beijing, Atmos. Pollut. Res., 7, 260-267, 10.1016/j.apr.2015.10.006, 2016b.

Zhou, J. B., Xiong, Y., Xing, Z. Y., Deng, J. J., and Du, K.: Characterizing and sourcing ambient PM2.5 over key emission regions in China II: Organic molecular markers and CMB modeling, Atmospheric Environment, 163, 57-64, 10.1016/j.atmosenv.2017.05.033, 2017.

816 Zhu, C., Kawamura, K., and Fu, P.: Seasonal variations of biogenic secondary organic
817 aerosol tracers in Cape Hedo, Okinawa, Atmospheric Environment, 130, 113-119,
818 10.1016/j.atmosenv.2015.08.069, 2016.
819 Zhu, Y., Yang, L., Kawamura, K., Chen, J., Ono, K., Wang, X., Xue, L., and Wang, W.:
820 Contributions and source identification of biogenic and anthropogenic
821 hydrocarbons to secondary organic aerosols at Mt. Tai in 2014, Environmental
822 Pollution, 220, 863-872, 10.1016/j.envpol.2016.10.070, 2017.

Table

Table 1. Summer $PM_{2.5}$ mass concentrations in Beijing from 2008-2016, average ± standard deviation (μg m^{-3}).

Year/Month	2008/07	2009/07	2010/05	2016/05-06	2016/05-06
Site	PKUERS	PKUERS	PKUERS	CP	PKUERS
	(μg m^{-3})	(μg m^{-3})	(μg m^{-3})	(μg m^{-3})	(μg m^{-3})
$PM_{2.5}$	92.3±44.7	88.2±52.3	62.7±36.5	43.0±17.5	45.5±19.8
OC	10.4±2.9	8.5±2.5	8.9±4.5	8.9±3.2	11.0±3.7
EC	3.3±1.5	2.5±0.9	2.1±1.1	0.7±0.5	1.8±1.0
SO_4^{2-}	35.6±24.7	25.5±18.6	11.8±9.8	7.9±5.7	4.7±3.4
NO_3^-	7.9±6.9	17.8±13.2	10.0±11.2	3.4±3.3	2.4±2.3
NH_4^+	15.2±11.3	13.5±8.4	5.9±5.9	4.6±3.0	3.5±3.5
Ref.	(Guo et al., 2012)	(Zheng et al., 2016a)	(Zheng et al., 2016a)	This study	This study

Figure captions

Fig. 1 Concentrations of organic carbon from primary and secondary organic sources at (a) CP and (b) PKUERS as well as their contributions to the measured organic carbon at (c) CP and (d) PKUERS (%).

Fig. 2 Comparison of the sources at PKUERS between 2016 and 2008

Fig. 3 Particle sources from different air mass origins

Fig. 4 Correlations between SOC and different influencing factors (a)-(b) ozone, (c)-(d) temperature, (e)-(f) water and (g)-(h) H^+ concentration (i)-(j) sulfate concentration

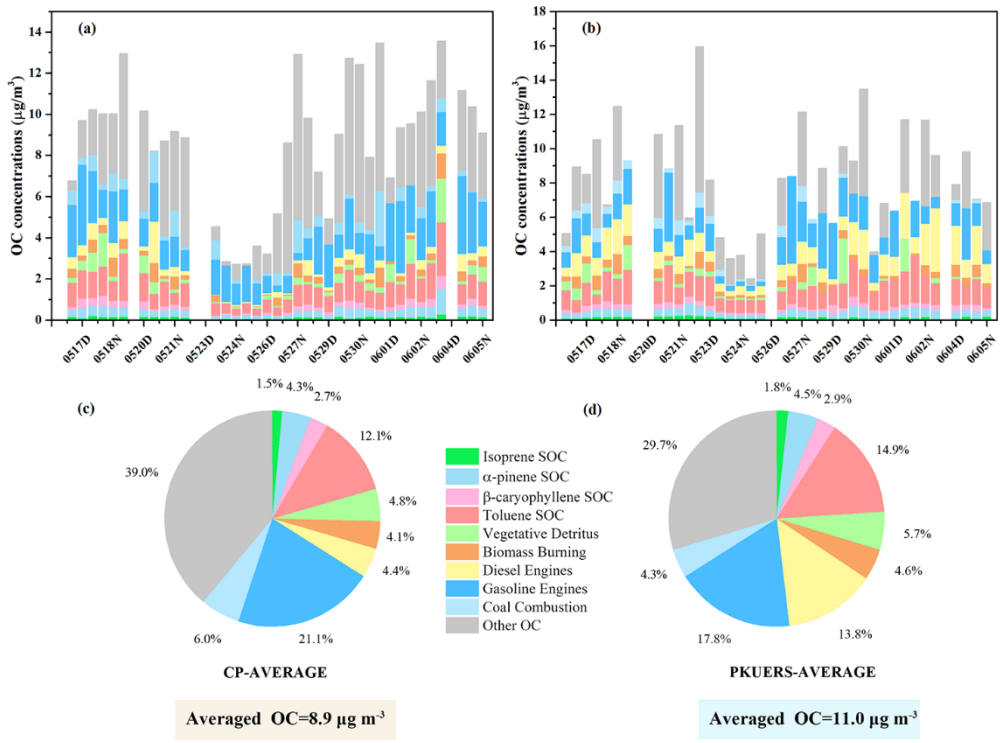

Fig. 1 Concentrations of organic carbon from primary and secondary organic sources at (a) CP and (b) PKUERS as well as their contributions to the measured organic carbon at (c) CP and (d) PKUERS (%).

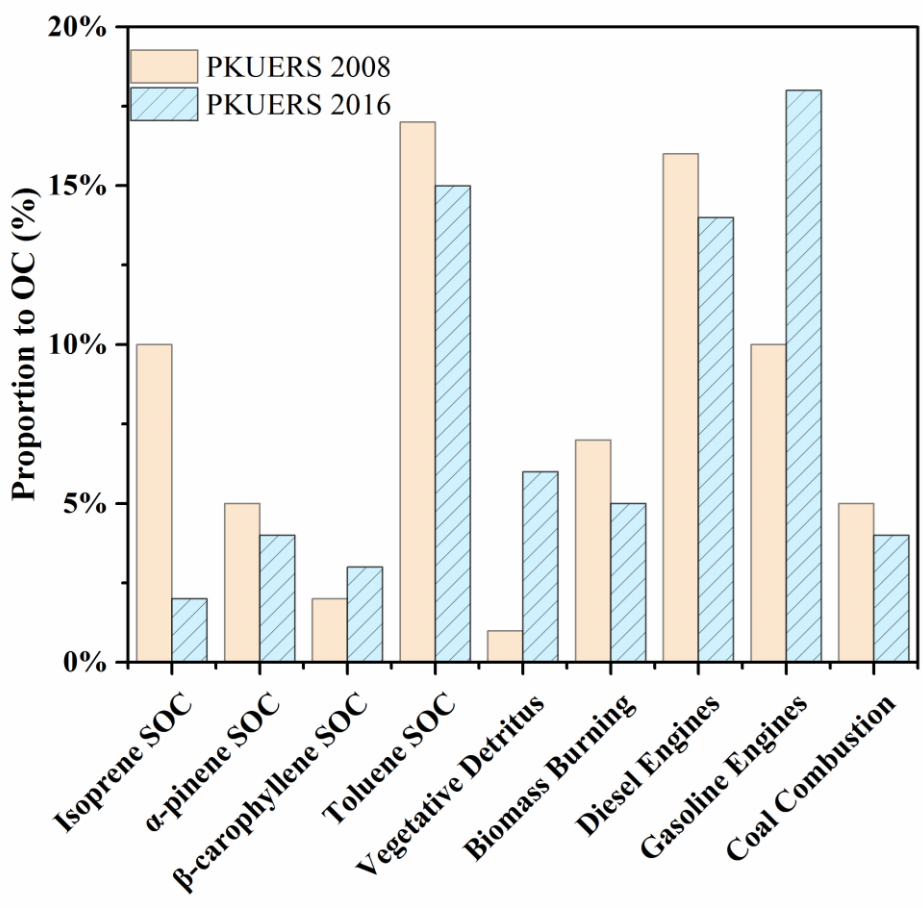

Fig.2 Comparison of the sources at PKUERS between 2016 and 2008 (Guo et al. 2012)

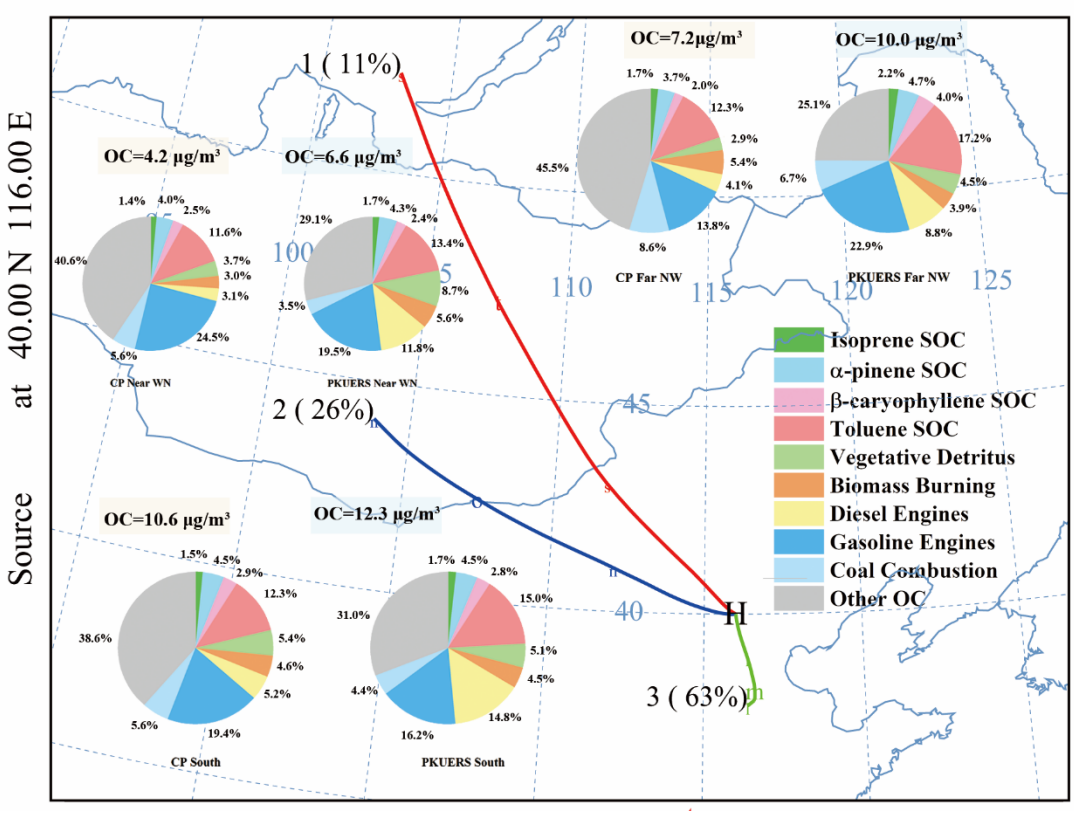

Fig. 3 Particle sources from different air mass origins

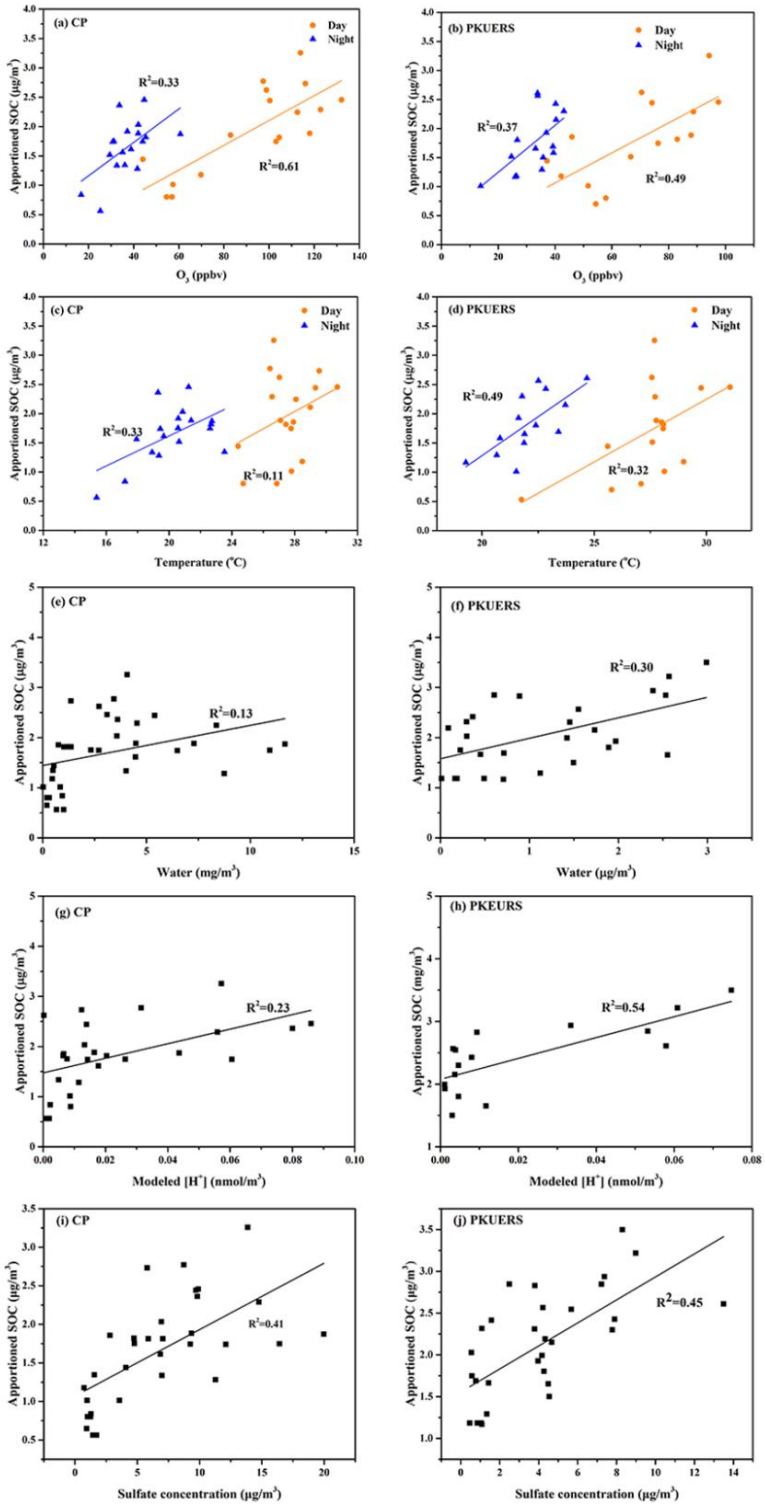

Fig. 4 Correlations between SOC and different influencing factors (a)-(b) ozone, (c)-(d) temperature, (e)-(f) water and (g)-(h) H^+ concentration (i)-(j) sulfate concentration